Mat. Res. Soc. Symp. Proc. Vol 615 © 2000 Materials Research Society

Observation of Long-Range Orientational Ordering in Metal Films Evaporated at Oblique Incidence onto Glass

David L. Everitt[1], X. D. Zhu*[1], William J. Miller[2], and Nicholas L. Abbott[3]

* to whom correspondence should be made (xdzhu@physics.ucdavis.edu)
[1]Department of Physics, University of California at Davis, Davis, California 95616
[2]Department of Chemical Engineering and Materials Science, University of California at Davis, Davis, California 95616
[3]Department of Chemical Engineering, University of Wisconsin, Madison, Wisconsin 53706

ABSTRACT

We studied long-range orientational ordering in polycrystalline Au films (10 nm - 30 nm) that are evaporated at oblique incidence onto a glass substrate at room temperature. By measuring the averaged optical second-harmonic response from the films over a 6-mm diameter region, we observed a transition from the expected in-plane mirror symmetry at 10 nm to a surprising three-fold in-plane rotational symmetry at 30 nm. X-ray pole figure analysis performed on these films showed the strong <111> fiber texture typical of fcc films, but with a restricted, three-fold symmetric, distribution of crystallite orientations about the fiber axis.

INTRODUCTION

Thin polycrystalline films are used in a wide range of industrial applications, from magnetic storage and read-head media to anchoring and control of functional molecular overlayers in applications such as flat panel displays [1]. Properties of a film depend–among other things–on the film's texture, that is, the distribution of crystalline grain orientations within the film.

Vapor-phase depositions often lead to crystalline grains terminated with Miller-index planes that have the minimum surface energy and that are more or less parallel to the substrate surface. Such films are termed to have out-of-plane textures (fiber texture) [2]. For many metals, the plane parallel to the substrate is the close-packed atomic plane. For example, a {111} plane is usually parallel to the substrate in face-centered cubic (fcc) metals. Note that for consistency of notation we will define this particular {111} plane to be the (111) plane. When the deposition is at an oblique angle or when a thin film is bombarded with ions at an oblique angle during growth, the resultant crystalline grains may also develop a preferred in-plane orientation with respect to the incidence plane of the deposition or bombardment [4,5,6]. Such films are termed to have both out-of-plane and in-plane textures (sheet texture). In-plane textures can be very desirable since they may provide an easy axis of magnetization in the surface plane for magnetic films. They may also cause molecular overlayers to have a preferred orientation with respect to the in-plane texture [1,7]. Recently Gupta and Abbott observed that on an obliquely deposited gold film (on fused silica) covered with an *n*-alkanethiol self-assembled monolayer (SAM), a liquid crystal overlayer consisting of 5'-pentylcyanobiphenyl (5CB) was aligned either along the in-plane direction of the deposition or perpendicular to it, depending on whether the alkane chain of the *n*-alkanethiol has an even or odd number of CH_2 groups [8]. Such an odd-even effect may conceivably be related to an in-plane texture if the latter is present in the gold film.

In this work, by measuring the optical second-harmonic response and the X-ray pole figures, we find that an obliquely deposited gold film on fused silica indeed develops an in-plane texture as well as an out-of-plane texture when the thickness increases from 10 nm to 30 nm. Though not discussed in this paper due to space limitations, the development of a preferred in-plane orientation can be attributed to a self-shadowing effect and thus is expected to occur in other metal thin films.

EXPERIMENT AND RESULTS

The gold films are prepared on fused silica substrates at room temperature in an electron beam evaporator. The evaporator chamber has a base pressure of 4×10^{-6} torr. The substrates are cleaned with the same method as reported by Skaife and Abbott [9]. The gold deposition rate is roughly 0.02 nm/sec. To help the gold films to adhere to the fused silica surface, we first deposit a 1-nm titanium (Ti) layer as the buffer. For obliquely deposited gold films, the gold flux is incident at 50° from the substrate normal and along a fixed azimuth. For comparison, we have also made "uniformly deposited" gold films by varying the incidence polar angle from 0° to 70° and the incidence azimuth from 0° to 360° during deposition. Conventional powder X-ray diffraction measurements show that the polycrystalline grains in both obliquely deposited and "uniformly deposited" gold films have <111> fiber texture. We have also measured the X-ray pole figures of these gold films with a Huber Pole Figure Goniometer. The pole figures give the angular distribution of the polycrystalline grain orientation [2]. The results show that (1) the (111) planes for the 30-nm obliquely deposited films are tilted by $\theta \sim 5°$ towards the deposition flux, while the (111) planes for the 30-nm "uniformly deposited" films are parallel to the substrate surface; (2) the polycrystalline grains in the 30-nm obliquely deposited films seem also to have developed a preferred in-plane orientation such that one of the three <110> axes in the (111) plane is perpendicular to the incidence plane of the deposition. Unfortunately the signal-to-noise ratio in the pole figure measurements was not high enough to exhibit the in-plane texture distinctly. The in-plane texture and how it evolves as the film thickness increases are much better exhibited in the optical second-harmonic response of the films.

The measurements of the optical second-harmonic generation (SHG) from the gold films are performed in air. We use 20-picosecond optical pulses at $\lambda_\omega = 532\ \text{nm}$ as the fundamental beams. The optical pulses are obtained by frequency-doubling the output of a Nd:YAG laser with a repetition rate of 10 Hz. In Fig. 1, we show the sketch of the optical set-up.

We choose the substrate surface (also the gold film surface) as the x-y plane and the incidence plane of the optical beams as the x-z plane with the z-axis pointing into the substrate. We employ a co-planar, sum-frequency generation geometry such that one fundamental beam (*p-polarized* with a single pulse energy of 0.1 mJ over an area of 0.3-cm^2) is incident at 22° from one side of the substrate normal while the other fundamental beam (also *p-polarized* with a single pulse energy of 0.3 mJ over an area of 0.4-cm^2) is incident at 45° from the opposite side. We detect the *p-polarized* optical second harmonics (at $\lambda_{2\omega} = 266\ \text{nm}$) in reflection direction at 10° from the substrate normal.

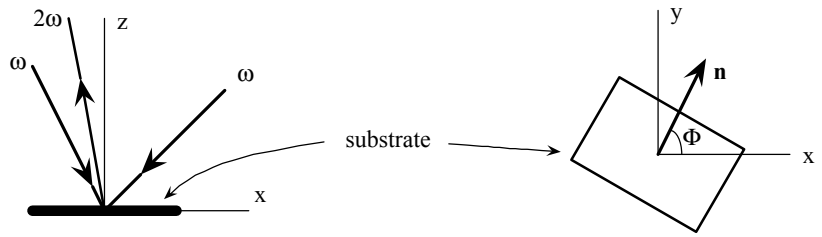

Fig. 1 The geometry of the SHG from an obliquely deposited gold film. The substrate surface coincides with the x-y plane. Two *p-polarized* excitation beams at ω are incident in the x-z plane: one at 22° from one side of the substrate normal and the other at 45° from the opposite side. The reflected SHG at 2ω is emitted at 10° from the substrate normal. The gold flux is deposited onto the substrate at 50° from the normal. The unit vector **n** denotes the projected direction of the deposition in the x-y plane. Φ is the azimuthal angle between **n** and the x-axis.

In this geometry, the measured optical second harmonics is predominantly generated by the x-component of the nonlinear polarization $P_x(2\omega)$ in the gold film. $P_x(2\omega)$ is sensitive to the in-plane structure of the film [10].We measure the azimuthal dependence by rotating the gold film about the substrate normal over 360° at a step size of 10°. Let **n** be a unit vector in the x-y plane along the projected direction of the deposition. The azimuthal angle Φ is defined as the angle between **n** and the x-axis.

In Fig. 2, we display the SHG signal versus Φ from obliquely deposited gold films of three different thicknesses: 10 nm [Fig. 2(a)], 20 nm [Fig. 2(b)], and 30 nm [Fig. 2(c)]. The SHG signal originates from the electric quadrupole and magnetic dipole responses of the gold film [10]. As a result of the attenuation at the fundamental and the SH frequencies, the SHG signal and its azimuthal dependence comes from the topmost 10 nm of the film and the contribution from the 1-nm Ti buffer layer can be neglected. This is consistent with our observation that the averaged SHG signal is roughly the same at all three film thicknesses. For the 10-nm gold film, the SHG has only a mirror plane coinciding with the incidence plane of the deposition as one would expect from the geometry of deposition. It has a minimum at $\Phi = 0^\circ$ and a broad maximum at $\Phi = 180^\circ$. At the film thickness of 20 nm, a small peak emerges at $\Phi = 0^\circ$ while the maximum at $\Phi = 180^\circ$ shrinks. At the film thickness of 30 nm, the azimuthal dependence has evolved to having a three-fold rotation axis just like the SHG from a single crystalline Au(111) [11]. The peak at Φ = 180° is noticeably smaller than the peaks at Φ = 60° and 300°. It seems that at 20 nm the evolution of the azimuthal dependence is incomplete. For comparison, the SHG from the "uniformly deposited" films is azimuthally isotropic, indicating that the in-plane orientations of the polycrystalline grains in these films are random.

The presence of a 3-fold rotational axis in SHG from 30-nm obliquely deposited gold films, after an average over an area of 0.3 cm^2, is indicative of a preferred azimuthal orientation of the polycrystalline grains in these films.

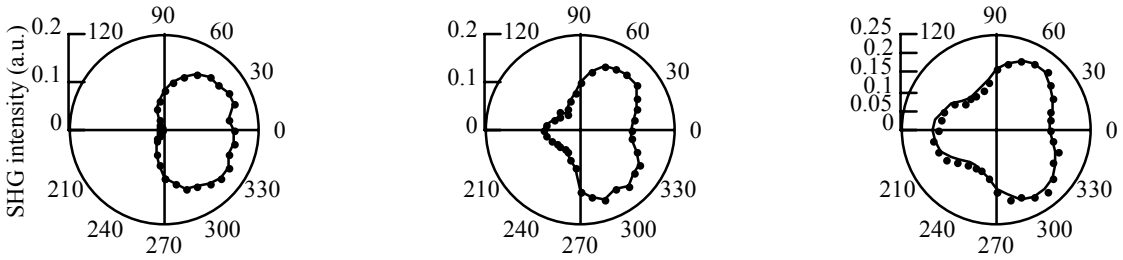

Fig. 2 Azimuthal dependence of the *p-polarized* SHG intensity (in unit of photon counts per pulse) from obliquely deposited gold films vs. the film thickness: (a) 10 nm; (b) 20 nm; (c) 30 nm. The solid line shown in (c) is the best fit of a function $\beta\,(1-\gamma\cos 3\Phi+\eta\cos\Phi)^2$ to the data with $\beta = 0.15$, $\gamma = 0.23$ and $\eta = 0.14$.

Our SHG measurement should be compared to the measurement of a non-resonant optical sum-frequency generation from a single crystal Au(111) by Yeganeh and coworkers [11]. Similar to Fig. 2(c), these authors observed a 3-fold rotation axis with the SHG maxima appearing at 60°, 180°, and 300°. As we will show shortly, the asymmetry of the three SHG peaks in Fig. 2(c) can be attributed to a small tilt of the [111] axes of the gold grains towards the deposition flux.

In our case, the optical second harmonics is predominantly generated by the x-component of the nonlinear polarization $P_x(2\omega)$ in the topmost 10-nm layer of the gold films. It is an average of the nonlinear polarization over many polycrystalline grains. From a single crystalline grain (e.g., the j-th grain), the nonlinear polarization $P_{x,j}(2\omega)$ has an isotropic part $P_{x,j}^{\text{isotropic}}(2\omega)$ and an anisotropic part $P_{x,j}^{\text{anisotropic}}(2\omega)$ [10]. Let θ be the tilt angle of the [111] axis from the substrate normal. Let ϕ_j be the angle between **n** (see Fig. 1) and one of the [211] axes in the terminating facet plane. For a small tilt angle θ, it can be shown that $P_{x,j}^{\text{anisotropic}}(2\omega) \sim \left[-\cos 3\left(\Phi-\phi_j\right)+\left(3/\sqrt{2}\right)\theta\cos\left(\Phi-\phi_j\right)\right]$ and consequently

$$P_x(2\omega)=\sum_j P_{x,j}(2\omega)\sim\sum_j\left[1-\alpha\cos 3\left(\Phi-\phi_j\right)+\alpha\left(3/\sqrt{2}\right)\theta\cos\left(\Phi-\phi_j\right)\right] \tag{1}$$

The total SHG signal as a function of Φ is given by $S(\Phi)\sim\left|P_x(2\omega)\right|^2$. α is a constant determined by the geometry of the experimental set-up. Equation (1) is equivalent to an ensemble average over a distribution of the azimuthal orientations around $\phi = 0^\circ$ for those polycrystalline grains within a macroscopic area of 0.3-cm^2. As a result, we have

$$S(\Phi)\sim\left|P_x(2\omega)\right|^2\sim\left|1-\alpha\langle\cos 3\phi\rangle\cos 3\Phi+\alpha\left(3/\sqrt{2}\right)\theta\langle\cos\phi\rangle\cos\Phi\right|^2 \tag{2}$$

If the azimuthal orientations of the grains are random (as one would expect of films deposited on amorphous substrates like fused silica) such that ϕ varies from - 60° to + 60°, $\langle \cos 3\phi \rangle$ vanishes and the resultant $S(\Phi)$ only have a weak mirror plane given by the $\alpha\left(3/\sqrt{2}\right)\theta\langle\cos\phi\rangle\cos\Phi$ term. If the tilt angles of the fiber axes are also randomly distributed about $\theta = 0°$, the resultant $S(\Phi)$ becomes isotropic as we found for "uniformly deposited" gold films. If instead there is a preferred orientation along $\phi = 0^{\circ}$ so that ϕ varies over a significantly narrower range than 120°, $\langle \cos 3\phi \rangle$ survives the ensemble average and $S(\Phi)$ has a 3-fold rotation axis in addition to a weak asymmetry coming from the tilt angle. This is what we observed for obliquely deposited gold films with thicknesses over 10 nm. The data in Fig. 2(c) is best fit to Equation (2) (solid line) by assuming that *one of the <110> axes in the (111) plane is perpendicular to the incident plane of the deposition* and with $\left(3/\sqrt{2}\right)\theta\langle\cos\phi\rangle/\langle\cos 3\phi\rangle = +0.6$.

The observed in-plane texture and tilt angle θ towards the deposition direction for the polycrystalline grains in an obliquely deposited gold film may have a significant effect on the macroscopic alignment of the terminal methyl groups of an *n*-alkanethiol self-assembled monolayer (SAM) on such a film [8]. It is known that the methyl groups of a *(2m)*-alkanethiol SAM on Au(111) are more or less oriented along the substrate normal [15]. On an obliquely deposited gold film with the (111) axes tilted towards the deposition direction, the methyl groups of a *(2m)*-alkanethiol SAM on these facets would be also tilted towards the deposition direction. On the other hand, the methyl groups of a *(2m+1)*-alkanethiol SAM on Au(111) are tilted along an in-plane <110> axis [15]. On an obliquely deposited gold film, one of the <110> axes in the (111) plane is perpendicular to the incidence plane of the deposition and the other two <110> axes are at an angle of 60° from the plane of the deposition. On these facets, the orientations of the methyl groups will be determined both by the orientation of the <110> axes and the tilt of the [111] axes. We speculate that short-ranged interactions between the oriented methyl groups and liquid crystal overlayers may provide part of the explanation, at least, for the previously reported effects on liquid crystals of *n*-alkanethiols with odd and even numbers of CH_2 groups on obliquely deposited gold films [8]. We caution, however, that the orientations of the methyl groups on these substrates need to be determined directly using techniques such as the infrared-visible sum-frequency generation [16].

CONCLUSION

In conclusion, we have shown that a thin gold film obliquely deposited on fused silica (with 1-nm Ti buffer layer) develops an in-plane texture as well as an out-of-plane texture. The out-of-plane texture is such that the (1) the polycrystalline grains have (111) planes parallel to the substrate; and (2) the [111] axes are tilted by a few degrees towards the deposition direction. The in-plane texture is characterized by a preferred azimuthal orientation of the polycrystalline grains with one of the <110>] axes in the (111) plane oriented perpendicular to the incidence plane of the deposition. Such in-plane and out-of-plane textures can find desirable applications in magnetic thin films and in anchoring molecular overlayers as soft-hard material interfaces.

ACKNOWLEDGEMENTS

This work was supported by National Science Foundation under NSF-DMR-9808677 and in part under NSF-DMR-9818483. We thank Professor Wenk for performing the X-ray pole figure measurements reported in this work. N.L.A. acknowledges the support by the Office of Naval Research (Presidential Early Career Award for Science and Engineering) and by the Center for Nanostructured Interfaces (NSF-DMR-9632527) at University of Wisconsin-Madison.

REFERENCES

1. J. Cognard, *Alignment of Nematic Liquid Crystals and Their Mixture* (Gordon and Breach, London, 1982).
2. H.J. Bunge, *Texture Analysis in Materials Science* (Butterworths, Toronto, 1982).
3. T.G. Knorr and R.W. Hoffman, Phys. Rev. **113**, 1039 (1959).
4. T.C. Huang, J.-P. Nozieres, V.S. Speriosu, H. Lefakis, and B.A. Gurney, Appl. Phys. Lett. **60**, 1573 (1992).
5. J.M. Alameda, F. Carmona, F.H. Salas, L.M. Alvarez-Prado, R. Morales, G.T. Perez, J. Magn. Magn. Mater. **154**, 249 (1996); K. Itoh, *ibid.* **95**, 237 (1991); K. Okamoto, K. Itoh, and T. Hashimoto, *ibid.* **87**, 379 (1990); Z. Shi and M.A. Player, Vacuum **49**, 257 (1998).
6. J.M.E. Harper, K.P. Rodbell, E.G. Colgan, and R.H. Hammond, Mat. Res. Soc. Symp. Proc. **472**, 27 (1997).
7. M.B. Feller, W. Chen, and Y.R. Shen, Phys. Rev. **A 43**, 6778 (1991).
8. V.K. Gupta and N.L. Abbott, Phys. Rev. **B** *Rapid Commun.*, R4540 (1996).
9. J.J. Skaife and N.L. Abbott, Chem. Mater. **11**, 612 (1999).
10. H.W.K. Tom, T.F. Heinz, and Y.R. Shen, Phys. Rev. Lett. **51**, 1983 (1983); H.W.K. Tom, Ph.D. Thesis, University of California, 1984, p. 144.
11. M.S. Yeganeh, S.M. Dougal, R.S. Polizzotti, and P. Rabinowitz, Phys. Rev. Lett. **74**, 1811 (1995).
12. K.H. Hansen, T. Worren, S. Stempel, E. Lægsgaard, M. Bäumer, H.-J. Freund, F. Besenbacher, and I. Stensgaard, Phys. Rev. Lett. **83**, 4120 (1999).
13. W. Mahoney, S.T. Lin, and R.P. Andres, in *Evolution of Thin Film and Surface Structure and Morphology,* Materials Research Society Symposium Proceedings, Vol. **355**, edited by B.G. 14.O.P. Karpenko, J.C. Bilello, and S.M. Yalisove, J. Appl. Phys. **82**, 1397 (1997).
15. P. Fenter, A. Eberhardt, P. Eisenberger, Science **266**, 1216 (1994); P. Fenter, A. Eberhardt, K.S. Liang, and P. Eisenberger, J. Chem. Phys. **106**, 1600 (1997).
16. X. Wei, X. Zhuang, S.-C Hong, T. Goto, and Y.R. Shen, Phys. Rev. Lett. **82**, 4256 (1999).